VIIRS CLOUD MASK (VCM)

VISIBLE/INFRARED IMAGER/RADIOMETER SUITE ALGORITHM THEORETICAL BASIS DOCUMENT

Version 5, Revision 1: May 2002

Bonnie Reed

RAYTHEON SYSTEMS COMPANY

Information Technology and Scientific Services

4400 Forbes Boulevard

Lanham, MD 20706

SBRS Document #: Y2412

EDR: CLOUD MASK

Doc No: Y2412

Version: 5

Revision: 1

	Function	Name	Signature	Date
PREPARED BY	EDR DEVELOPER	B. REED		5/21/02
APPROVED BY	RELEVANT LEAD	R. SLONAKER		5/22/02
APPROVED BY	CHIEF SCIENTIST	S. MILLER		5/23/02
RELEASED BY	ALGORITHM LEAD	P. KEALY		5/24/02

TABLE OF CONTENTS

Raytheon

LIST OF FIGURES

Raytheon

LIST OF TABLES

GLOSSARY OF ACRONYMS

APOLLO	AVHRR Processing Scheme Over cloud Land and Ocean
ATBD	Algorithm Theoretical Basis Document
AVHRR	Advanced Very High Resolution Radiometer
AVIRIS	Airborne Visible Infrared Imaging Spectrometer
BT	Brightness Temperature
BTD	Brightness Temperature Difference
CLAVR	Clouds from AVHRR
CMIS	Conical Scanning Microwave Imager/Sounder
CrIS	Cross-track Infrared Sounder
EDC	EROS Data Center
EDR	Environmental Data Record
EROS	Earth Resources Observation System
FOV	Field of View
GAC	Global Area Coverage
HIRS	High Resolution Infrared Radiation Sounder
HSR	Horizontal Spatial Resolution
IR	Infrared
LAC	Local Area Coverage
LUT	Look-Up Table
MAS	MODIS Airborne Simulator
MCM	MODIS Cloud Mask
MODIS	Moderate Resolution Imaging Spectroradiometer
MODTRAN	Moderate Resolution Atmospheric Radiance and Transmission Model
NASA	National Aeronautics and Space Administration
NCEP	National Center for Environmental Prediction
NIR	Near Infrared
NOAA	National Oceanic and Atmospheric Administration
NPOESS	National Polar-orbiting Operational Environmental Satellite System
Ref	Reflectance
RGB	Red-Green-Blue
SDR	Sensor Data Record
SERCAA	Support of Environmental Requirements for Cloud Analysis and Archive
SRD	Sensor Requirements Document
SUCCESS	Subsonic Aircraft Contrail and Cloud Effects Special Study
TOA	Top-of-Atmosphere

USGS	United States Geological Survey
UV	Ultraviolet
UW	University of Wisconsin
VCM	VIIRS Cloud Mask
VIIRS	Visible/Infrared Imager/Radiometer Suite

Raytheon

ABSTRACT

Identifying pixels as either cloudy or clear is an essential component of the National Polar-orbiting Operational Environmental Satellite System (NPOESS) Visible/Infrared Imager Radiometer Suite (VIIRS). The VIIRS Cloud Mask (VCM) technique incorporates a number of cloud detection tests that determine whether a pixel is obstructed by a cloud. If a cloud is detected, the VCM indicates whether its phase is water, ice, or mixed. Additionally, the VCM specifies whether aerosols, fire, or shadows are detected within the pixel field of view (FOV). A spatial uniformity test is also performed on the scene. The VCM algorithm first determines a processing path for each pixel. The processing path indicates day or night, sun glint, land (desert or non-desert), water (inland or sea), coastline, and snow/ice background. After the processing path is established, the VCM algorithm conducts a series of threshold and ratio tests using solar reflectance. The algorithm also involves threshold and difference tests using the thermal Brightness Temperatures (BT). The threshold values for the various tests are dependent upon the dominant regional classification, or surface type, of the pixel. The tests applied to generate the VCM have a heritage from the Advanced Very High Resolution Radiometer (AVHRR) (Clouds from AVHRR [CLAVR], Stowe *et al*., 1995) and the Moderate Resolution Imaging Spectroradiometer (MODIS) (Ackerman *et al*., 1997). Each test returns a clear or cloudy result with an associated clear sky confidence level. Analogous to the MODIS Cloud Mask, the VCM groups its cloud confidence tests into five categories. The minimum clear sky confidence from individual members represents the clear sky confidence for that group and the product of all the group clear sky confidences is used to determine the overall clear sky confidence value. After the cloud confidence is determined, the VCM tests the pixel for aerosols, shadows, and fires, and then performs a spatial uniformity test. VIIRS cloud, aerosol, land, ocean, surface temperature, and snow/ice Environmental Data Records (EDRs) use the VCM as required input.

<div align="center">

1.0   INTRODUCTION

</div>

1.1   PURPOSE

This Algorithm Theoretical Basis Document (ATBD) describes the algorithm used to retrieve the Cloud Mask IP for the VIIRS instrument on the NPOESS. Specifically, this document identifies the sources of input data required for retrieval, provides the physical theory and mathematical background underlying the use of this information in the retrievals, includes implementation details, and describes assumptions and limitations of the proposed approach.

1.2   SCOPE

This document covers the algorithm theoretical basis for the cloud mask product of VIIRS on NPOESS. The VCM solution was developed using the MODIS and AVHRR cloud detection algorithm heritages.

Section 1 describes the purpose and scope of this document. Section 2 is an overview of the cloud mask. The theoretical description and implementation of the algorithm are described in Section 3, and the assumptions and limitations of the approach are summarized in Section 4. References for citations in the text are listed in Section 5.

1.3   VIIRS DOCUMENTS

This document contains references to other VIIRS documents. These are given in italicized brackets, e.g., *[Y2412]* CLOUD MASK. The VIIRS documents cited in this document are listed below:

[PS154640-102]	Performance Specification Algorithm Specification for the VIIRS
[Y2388]	VIIRS Software Development Plan
[Y2469]	VIIRS Context Software Architecture
[Y2470]	VIIRS Data Interface Control Document

1.4   REVISIONS

This is version five, revision 1 of this document dated May 2002. The original version of this document was dated September 1998.

2.0   EXPERIMENT OVERIVEW

2.1   OBJECTIVE OF VIIRS CLOUD MASK

The objective of the VCM is to determine whether clouds or optically thick aerosol obstruct a given view of the Earth surface. The VCM also determines the cloud phase and whether a clear scene is contaminated by a shadow. The VCM is defined as the pixel level flag that indicates when a cloud intersects a line segment extending between the sensor and a given area of the Earth's surface. The VCM operates at a moderate pixel resolution (750 m), and an imagery pixel resolution (375 m). Input to the cloud mask algorithm is assumed to be calibrated and navigated VIIRS radiance data, ancillary data, and auxiliary data. Additionally, the VIIRS data are assumed to meet instrument specifications so that no accommodation for striping or poor navigation is required.

Our approach to the VCM is for each pixel to provide a confidence flag that indicates how certain we are that the pixel is clear. The cloud mask algorithm must operate under the following restrictions: near-real time execution, limited computer storage, and simplicity so that many users can follow the algorithm path.

2.2   INSTRUMENT CHARACTERISTICS

The VIIRS bands used in the cloud mask algorithm are identified in Table 1. Additional details on the instrument design are provided in the VIIRS Experiment Overview *[V-0]*.

Table 1. VIIRS bands used in the VCM algorithm

VIIRS Band	Wavelength (μm)
M4	0.555
I1	0.64
M5	0.672
I2	0.865
M7	0.865
M8	1.24
M9	1.378
M10	1.61
M11	2.25
I4	3.74
M12	3.7
M13	4.05
M14	8.55
M15	10.7625
I5	11.45
M16	12.0125

2.3 HISTORICAL PERSPECTIVE

The VCM is essentially derived from the MODIS Cloud Mask (MCM) multi-channel cloud masking techniques, which in turn have their heritage in previously developed algorithms. The International Satellite Cloud Climatology Project (ISCCP) has developed cloud detection schemes using visible and infrared window radiances. The AVHRR Processing scheme Over cLoud Land and Ocean (APOLLO) cloud detection algorithm uses the five visible and infrared channels of the AVHRR. The NOAA Cloud Advanced Very High Resolution Radiometer (CLAVR) also uses a series of spectral and spatial variability tests to detect a cloud. Additionally, spatial coherence of infrared radiances in cloudy and clear skies has been used successfully in regional cloud studies.

The above algorithms are noted as they have been incorporated into current global cloud climatologies or have been run in an operational mode over long time periods. The VCM algorithm builds on this work, but has considerable advantage because it has multispectral information and conducts tests at the imagery and moderate resolutions. VIIRS has five Imagery resolution (375m) channels and sixteen Moderate resolution (750m) channels and both resolutions include channels in the visible, near-infrared, and thermal infrared.

Raytheon

3.0   ALGORITHM DESCRIPTION

3.1   PROCESSING OUTLINE

The current processing outline (see Figure 1) is based on the MODIS current operational approaches. The VCM uses VIIRS data and auxiliary data as input to produce a variety of output flags. The VCM output is used by many EDRs that are dependent on cloud masking. The VCM performs cloud tests at both the moderate resolution and at the higher imagery resolution.

VIIRS 375m Earth View SDR File

VIIRS 750m Earth View SDR File

VIIRS Gridded Surface Types – Olson IP

VIIRS Gridded Snow / Ice Cover IP

Global Ecosystem Map

Sea Surface Winds

2.3
Build VIIRS
Cloud
Mask IP
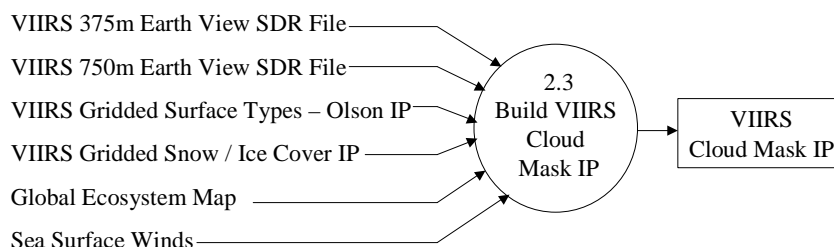
VIIRS
Cloud Mask IP

Figure 1. VCM Conceptual Design.

3.2   ALGORITHM INPUT

The algorithm requires ancillary information from the VIIRS instrument and auxiliary data from outside sources. All of the input data are explained in greater detail in this section.

Table 2. Ancillary & Auxiliary data inputs for the VCM

Input Data	Source of Data
VIIRS 375m Earth View SDR File	VIIRS
VIIRS 750m Earth View SDR File	VIIRS
VIIRS Gridded Surface Types-Olson IP	VIIRS
VIIRS Gridded Snow/Ice Cover IP	VIIRS
Global Ecosystem Map	USGS EDC
Sea Surface Winds	NCEP/CMIS

3.2.1   VIIRS Data

Input to the cloud mask algorithm is assumed to be calibrated and navigated VIIRS radiance data as well as geolocation, surface type, and snow/ice data.

3.2.1.1   VIIRS 375m Earth View SDR File

The VCM performs cloud detection tests at the imagery pixel resolution and therefore requires data from the VIIRS 375m Earth View SDR File. The VCM uses reflectance information from

bands I1 and I2 and BT information from bands I4 and I5. Imagery resolution geolocation parameters, terrain data, solar angles, and sensor angles are also obtained from this file.

3.2.1.2 VIIRS 750m Earth View SDR File

The VCM output is mainly based upon moderate pixel resolution tests and evaluations. Therefore, the VCM requires data from the VIIRS 750m Earth View SDR File. The VCM uses reflectance information from bands M4, M5, M7, M8, M9, M10, and M11 and BT information from bands M12, M13, M14, M15, and M16. Moderate resolution geolocation parameters, VIIRS grid information, terrain data, solar angles, and sensor angles are also obtained from this file.

3.2.1.3 VIIRS Gridded Surface Types – Olson IP

Various cloud detection tests have different thresholds over land than over water so the VIIRS Gridded Surface Types – Olson IP will be used by the VCM to create a land/water background flag. This IP will be utilized post-launch.

3.2.1.4 VIIRS Gridded Snow/Ice Cover IP

Spectrally, snow/ice and clouds have many similar features, therefore, the snow/ice map is needed to decide which cloud detection tests will be applied and to adjust thresholds of several tests. The previous 12-hour VIIRS Snow Cover EDR result will be used in conjunction with a reflectance based snow detection test to produce a snow/ice map. The snow/ice map will decrease the misclassification of snow/ice as clouds.

3.2.2 Non-VIIRS Data

The non-VIIRS data that the VCM uses is provided by several different sources and is described in the following subsections.

3.2.2.1 Global Ecosystem Map

Various land types possess different reflective properties. The reflective properties need to be known to properly develop and identify the correct thresholds to be applied in cloud tests. The USGS EROS Data Center (EDC) produces a Global Land Cover Characteristics map that includes classifications such as inland water, seawater, desert, land, forest, and coast. This map will be used to determine the background land type of each pixel at launch and will be used in conjunction with the VIIRS Gridded Surface Types – Olson IP when it is ready.

3.2.2.2 Sea Surface Winds

Sea surface winds need to be analyzed when determining sun glint. Therefore, sea surface wind data is needed to determine if sun glint is present over a water surface. Sea surface wind data will be obtained from NCEP sea surface forecast.

Raytheon

3.3 ALGORITHM OUTPUT

The output of the VCM algorithm will be 6 bytes (48 bits) for each moderate resolution pixel. The mask includes information about the processing path the algorithm took (e.g., land or ocean) and whether a view of the surface is obstructed. A potentially large number of applications will use the cloud mask and some algorithms will be more tolerant of cloud contamination than others. For example, some algorithms may apply a correction to account for the radiative effects of a thin cloud. In addition, certain algorithms may use spectral channels that are more sensitive to the presence of clouds than others.

To allow for the imprecise measurement of the real world and to accommodate a wide variety of applications, the mask is more than a simple yes/no decision. The cloud mask includes 4 levels of 'confidence' with regard to whether a pixel is thought to be clear as well as the results from different spectral tests. The bit structure of the cloud mask is described in Table 3 and a description of the bit fields follow.

Table 3. File specification for the 48-bit VCM

BYTE	Bit	Flag Description Key	Result
0	0-1	Cloud Mask Quality	00=Poor 01=Low 10=Medium 11=High
	2-3	Cloud Detection Result & Confidence Indicator	11 = Confident Cloudy 10 = Probably Cloudy 00 = Confident Clear 01 = Probably Clear
	4	Day / Night	0 = Night 1 = Day
	5	Snow / Ice Surface	1 = Snow/Ice 0 = No Snow/Ice
	6-7	Sun Glint	00 = None 01 = Geometry Based 10 = Wind Speed Based 11 = Geometry & Wind
1	0-2	Land / Water Background	000 = Land & Desert 001 = Land no Desert 010 = Inland Water 011 = Sea Water 101 = Coastal
	3	Shadow Detected	1 = Yes 0 = No
	4	Non Cloud Obstruction (Heavy Aerosol)	1 = Yes 0 = No
	5	Fire Detected	1 = Yes 0 = No
	6	Thin Cirrus Detection (Solar) (RM9)	1 = Cloud 0 = No Cloud
	7	Thin Cirrus Detection (IR) (BTM15-BTM16)	1 = Cloud 0 = No Cloud
2	0	IR Threshold Cloud Test (BTM15)	1 = Cloud 0 = No Cloud
	1	High Cloud (BTM12 - BTM16) Test	1 = Cloud 0 = No Cloud

BYTE	Bit	Flag Description Key	Result
	2	IR Temperature Difference Test (BTM14 - BTM15 & BTM15 - BTM16)	1 = Cloud 0 = No Cloud
	3	Temperature Difference Test (BTM15 - BTM12)	1 = Cloud 0 = No Cloud
	4	Temperature Difference Test (BTM12 – BTM13)	1 = Cloud 0 = No Cloud
	5	Visible Reflectance Test (RM5)	1 = Cloud 0 = No Cloud
	6	Visible Reflectance Test (RM7)	1 = Cloud 0 = No Cloud
	7	Visible Ratio Test (RM7/RM5)	1 = Cloud 0 = No Cloud
3	0-1	Adjacent Pixel Cloud Confident Value	11 = Confident Cloudy 10 = Probably Cloudy 00 = Confident Clear 01 = Probably Clear
	2-3	Cloud Phase	00 = Not Executed 01 = Water 10 = Ice 11 = Mixed
	4-7	Imagery Resolution BTD Test	From 1111 = All Cloudy To 0000 = None Cloudy
4	0-3	Cloud Imagery Resolution RI1 Test	From 1111 = All Cloudy To 0000 = None Cloudy
	4-7	Cloud Imagery Resolution RI2 Test	From 1111 = All Cloudy To 0000 = None Cloudy
5	0	Conifer Boreal Forest	1 = Yes 0 = No
	1	Spatial Uniformity Test	1 = Yes 0 = No
	2-7	SPARE	

3.3.1   Cloud Mask Quality

Since VIIRS produces a cloud mask in any situation, a quality flag is attached to the final cloud mask. This flag reflects the number of tests executed for a given processing path. The values range from zero (no tests were executed) to three (all tests were executed).

3.3.2   Cloud Detection Result & Confidence Indicator

Confidence flags convey strength of conviction in the outcome of the cloud mask algorithm tests for a given pixel. When performing spectral tests, as one approaches a threshold limit, the certainty or confidence in the outcome is reduced. Therefore, a confidence flag for each individual test, based upon proximity to the threshold value, is assigned for the FOV. The current scheme applies a linear interpolation between a confident cloudy threshold and a confident clear threshold for each spectral test.

Raytheon

The final determination is a combination of the confidences of all applied tests. The final cloud mask determination will be one of four results: confident cloudy, probably cloudy, probably clear, confident clear.

3.3.3 Day/Night

The solar zenith angle at the pixel latitude and longitude is used to determine if a daytime or nighttime cloud masking algorithm should be applied. Daytime algorithms, which include solar reflectance data, are constrained to solar zenith angles less than 85°.

3.3.4 Snow/Ice Surface

Certain cloud detection tests (e.g., visible reflectance tests) are applied differently in the presence of snow or ice. This bit indicates a processing path and, if set, it should not be interpreted that snow/ice is on the ground. In daytime conditions, the VCM will execute a reflectance based snow detection algorithm to check for snow surfaces. During the night, the VCM will use the VIIRS Gridded Snow Cover IP to identify snow covered pixels.

3.3.5 Land/Water Background

The surface type flag contains information concerning the processing path taken through the algorithm. There are five possible surface type processing paths: inland water, seawater, coast, desert land, and non-desert land.

Thresholds for the spectral tests are a function of surface background, land and water being the two most obvious. The VCM will read a Global Ecosystem map from the EROS Data Center as well as the VIIRS Gridded Surface Types – Olson IP (post launch) data to determine the land/water background for each pixel.

3.3.6 Sun Glint Flag

There is a justifiable concern that cloud detection will not be as reliable in glitter-contaminated regions. A classification as clear is probably correct, but a classification as cloudy may actually be due to the glitter effect as opposed to a cloud. Sun glint will be considered over both land and water areas. Land regions are included because spatially unresolved water bodies, snow, or recent rainfall can also cause sun glint. Sun glint will not prohibit the generation of a cloud mask, however solar channel threshold values need to be adjusted for sun glint contaminated pixels.

The first sun glint test checks the value of the reflected sun angle θ_r. If θ_r is between 0° and 36°, the sun glint flag will be set. Below is the formula for the reflected sun angle:

$$\cos\theta_r = \sin\theta\sin\theta_o\cos\phi + \cos\theta\cos\theta_o$$

$$\theta = SatelliteZenithAngle$$
$$\theta_{\circ} = SolarZenithAngle$$
$$\phi = SatelliteAzimuthAngle$$

The second sun glint test evaluates the sea surface winds and the solar geometry. Knowledge of sea surface winds is included in the sun glint test because surface winds can narrow the region in which sun glint may occur. Sun glint is identified when the slope of the water reflects the sun towards the satellite. If the water surface is disturbed by wind the sun is reflected from multiple spots on the surface. As the wind-rippled surface moves, so do individual glints of reflected sun. Therefore, the ensemble of glints produces a glitter pattern whose shape and size can be related to sea surface wind speed and the satellite viewing geometry. In the equation below, P represents the probability that the pixel is contaminated by sun glint due to sea surface wind speed (McClain and Yeh, 1994). Sun glint is identified when P > 1.5.

$$P = (1/\pi\sigma^2)\exp[-\tan^2\theta_N/\sigma^2]$$

$\theta = SatelliteZenithAngle$ $\sigma^2 = 0.003 + 0.00512(windspeed(m/s))$

$\theta_{\circ} = SolarZenithAngle$ $\cos 2\omega = \cos\theta\cos\theta_{\circ} + \sin\theta\sin\theta_{\circ}\cos(\phi - \phi_{\circ})$

$\phi = SatelliteAzimuthAngle$ $\theta_N = \cos^{-1}[\cos\theta + \cos\theta_{\circ}/2\cos\omega]$

$\phi_{\circ} = SolarAzimuthAngle$

3.3.7 Shadow Detected

Some land retrieval products are as sensitive to the presence of shadows as they are to contamination by thin clouds. The VIIRS Cloud Masking algorithm checks for the presence of a shadow on the ground whenever the cloud confidence is confident clear. Shadow detection is based on reflectance at M5, M7, M8, and M10.

Mountainous terrain can also cause shadows. These shadows would be directly calculable from digital elevation maps, solar geometry considerations, and the cloud mask. The first two considerations would indicate the FOVs where terrain shadow could occur; the last would determine whether sunlight is available to cause the shadow. The cloud mask will not separate shadows caused by terrain from those caused by clouds.

An example of the results of the VCM shadow detection algorithm is shown in Figure 2. The left hand panel is a 1.61 μm image, and the right hand panel represents the shadow detection algorithm. White regions are shadowed regions and dark regions represent cloudy or non-shadow scenes. The shadow grouping on the left portion of the image represents shadows caused by mountainous terrain and the shadows on the right portion of the image is a result of cloud cover.

1.61 μm   **VIIRS Cloud Mask**
                                                       Shadow Bit
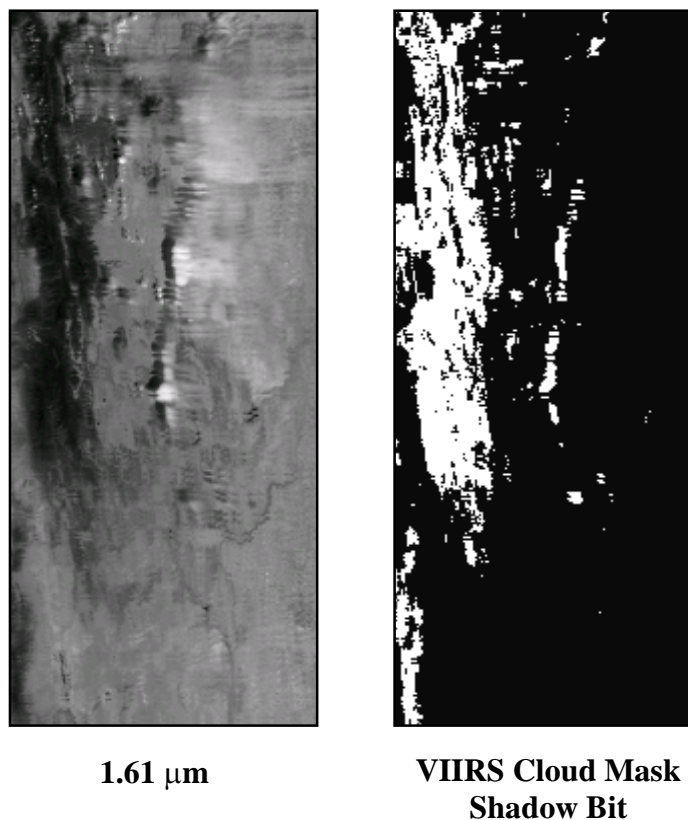
Figure 2. The VCM shadow detection result on MODIS data over the western United States.

3.3.8 Non-cloud Obstruction

A heavy aerosol laden atmosphere may result in pixel labeled probably clear. Certain simple tests may be constructed that can indicate that the pixel is contaminated with an aerosol and not a cloud. The non-cloud obstruction algorithm is of MODIS heritage and relies on Ref_{M11} and Ref_{M5}. The pixel is also checked for the presence of dust using BT_{M15}-BT_{M16}. If aerosols or dust is present, the non-cloud obstruction bit is set.

3.3.9 Fire Detected

The fire detection bit is modeled after the MODIS fire detection algorithm within the MCM. The fire detection scheme is executed over land and tests BT_{M12} and BT_{M12} - BT_{M15} against thresholds. If these tests indicate a fire, the pixel will be flagged.

3.3.10 Cloud Detection Tests

These bits represent the results of individual cloud detection tests. Each individual test is discussed in Section 3.5.

3.3.11 Cloud Adjacency

If a pixel is confident clear, the cloud confidence value of all eight adjacent pixels will be searched and the furthest value from confident clear will be reported. For edge of scan pixels, all available surrounding pixels will be searched.

3.3.12 Cloud Phase

If the cloud confidence is confident cloudy, probably cloudy, or probably clear, the VCM will determine the cloud phase as either ice, water, or mixed. Cloud phase is a front end to the VIIRS Precipitable Water EDR and all the VIIRS Cloud EDRs. It determines the processing path for the subsequent retrieval algorithms by categorizing clouds as water, ice or mixed. VIIRS Precipitable Water EDR and all the VIIRS Cloud EDRs process when the cloud confidence value is either confident cloudy, probably cloudy, or probably clear so a phase is determined under all of these conditions.

The VIIRS cloud phase algorithm follows the MODIS phase determination technique and evaluates BTM15 and the difference between bands M14 and M15. For each pixel, the first step is to use a simple threshold test to identify clouds that are sufficiently cold enough as ice clouds. Should the pixel be warmer than the initial ice-cloud threshold, it is tested further against BT_{M15} and BT_{M14}-BT_{M15}.

The VIIRS cloud phase algorithm was applied to MODIS data collected 1 June 2001 and a cloud phase result was obtained (see Figure 3). The distribution of BTs and BT differences corresponding to this scene is shown in Figure 4.
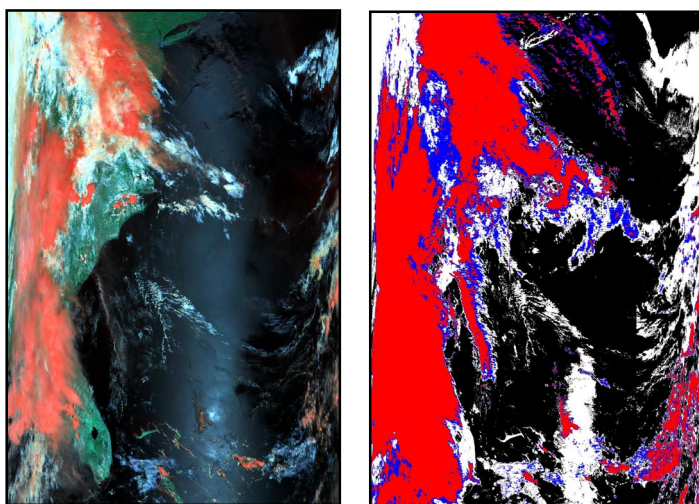
Figure 3. MODIS data collected 1 June 2001 from 1600 to 1605 UTC and the corresponding VCM Phase.
Left: RGB composite; Cold clouds are red, warm clouds are white, land is green and ocean is black.
Right: Ice clouds in red, water clouds in white, mixed clouds in blue, and confident clear pixel is black.

Raytheon
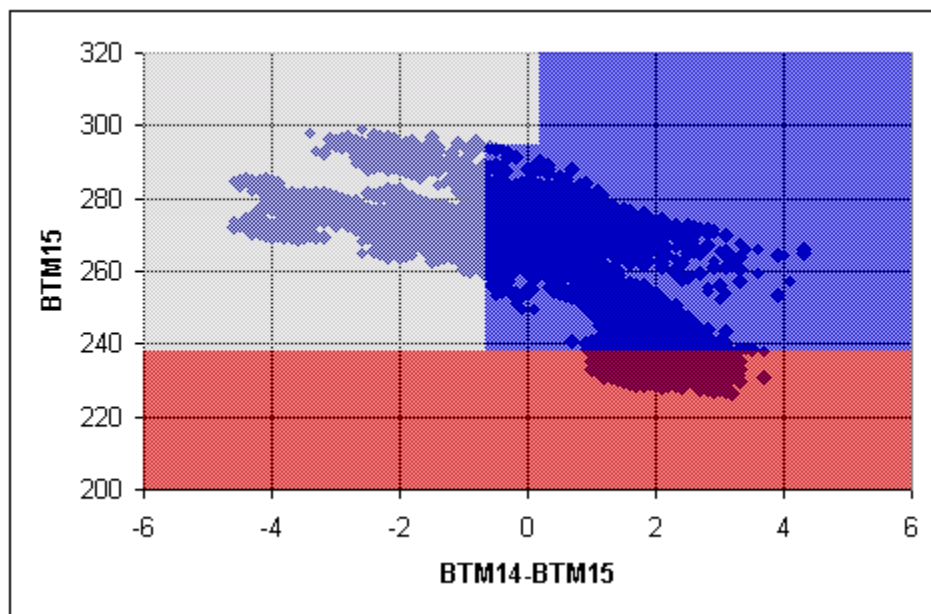
Figure 4. BTM15 vs. BTM14-BTM15 for the scene shown in Figure 3. Pixels located within the white area are classified as water clouds, the red area as ice cloud, and the blue area as mixed phase cloud.

3.3.13 Imagery Resolution Tests

The VIIRS Imagery resolution bands 'nest' in the moderate resolution bands. Figure 5 is an idealized picture of how the imagery bands relate to the moderate resolution pixel. This nesting allows the inclusion of an imagery resolution cloud mask along with the VCM output. The imagery resolution pixels, four of which are contained within a given moderate resolution pixel, undergo individual cloud detection tests. For the 48-bit output IP the four bits are ordered in reference to the satellite velocity vector, from the upper left quadrant to the lower right. The first bit is this upper left quadrant, the second bit is the upper right quadrant, the third bit is the lower left quadrant, and the fourth bit is the lower right quadrant. Cloud tests performed with these bands will be reported at the imagery resolution. Imagery band tests will be included in the cloud mask output, however; they are not used to determine the overall cloud confidence.
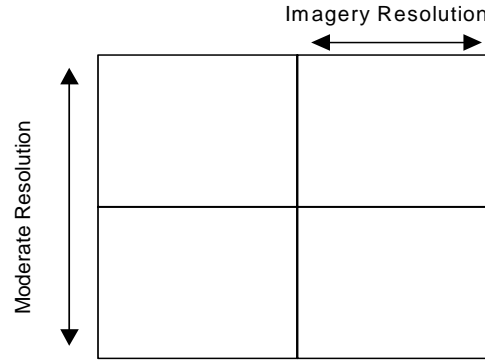
Figure 5. Depiction of the Nesting of the VIIRS Imagery Resolution Bands within the VIIRS Moderate Resolution Bands.

3.3.14 Conifer Boreal Forest

The Conifer Boreal Forest flag indicates whether a land pixel is of Conifer Boreal Forest type or not. This information is read from the USGS Global Ecosystem map and passed on to the Snow/Ice Module. The VCM classifies the Conifer Boreal Forest surface type as land no desert.

3.3.15 Spatial Uniformity

The infrared window spatial uniformity test is currently only executed over water surfaces. Most ocean regions are well suited for spatial uniformity tests; such tests may be applied with less confidence in coastal regions or regions with large temperature gradients (e.g., the Gulf Stream). If the cloud confidence result of a pixel is either probably cloudy or probably clear, the spatial uniformity test is implemented. This test evaluates BTM15 between the pixel of interest and all of the surrounding pixel brightness temperatures. If the difference of each surrounding pixel is less than 0.5, the scene is considered uniform and the bit is set. Surface temperature variability, both spatial and temporal, is larger over land than ocean, making land scene spatial uniformity tests difficult. Therefore, this test is not executed over land.

3.4 CLOUD CONFIDENCE DETERMINATION

The cloud detection tests rely on thresholds and thresholds are never global; there are always exceptions. For example, the ratio of reflectance at M7 to M5 identifies cloud for values in the range $0.9 < \text{Ref}_{M7}/\text{Ref}_{M5} < 1.1$. It seems unrealistic to label a pixel with $\text{Ref}_{M7}/\text{Ref}_{M5} = 1.09$ as cloudy, and a neighboring pixel with the ratio of 1.11 as non-cloudy. Rather, as one approaches the threshold limits, the certainty or confidence in the labeling becomes lower. An individual confidence flag is assigned to each single pixel test and is a function of how close the observation is to the thresholds. The individual confidence flags are combined to produce the final cloud mask flag for the VCM product.

The individual confidence flag will indicate a confidence level for each moderate resolution pixel. The initial FOV obstruction determination is an amalgamation of all confidence flags

resulting from the single pixel test results. The final cloud mask determination is a clear-sky confidence with one of four levels associated with it: confident clear, probably clear, probably cloudy and confident cloudy. This approach quantifies our confidence in the derived cloud mask for a given pixel.

Many cloud detection schemes have a single threshold for a given test. For example, if the visible reflectance of M7 over the ocean is greater than 5.5% then the pixel is set to cloudy. The VIIRS cloud masking is designed to provide information on how much confidence a user can place on the result. Each test is assigned a value between 0 and 1 representing increasing confidence in clear-sky conditions. Figure 6 is a graphical representation of how a confidence level is assigned for a spectral test. The abscissa represents the observation and the ordinate the clear-sky confidence level. In this test, an observation greater than a value of γ is determined to be a high confidence clear scene and assigned a value of 1. An observation with a value less than α is cloudy and assigned a confidence level of 0. These confident clear and confident cloudy thresholds, γ and α respectively, are determined from observations and/or theoretical simulations.

Values between α and γ are assigned a value between 0 and 1 (or 1 and 0). Assignment is based on a linear function. In the final cloud mask only four levels of confidence are provided; confident clear, probably clear, probably cloudy, and confident cloudy.

The β value in Figure 6 is the pass/fail threshold for a given test. Each test therefore has a minimum of three thresholds values: confident cloudy/probably cloudy, clear/cloudy, and confident clear/probably clear. Some tests, such as the visible ratio test, identify cloud if the observations fall within a given range (e.g., $0.9 < \text{Ref}_{M7}/\text{Ref}_{M5} < 1.1$). For these range tests there are six thresholds, three for each end.
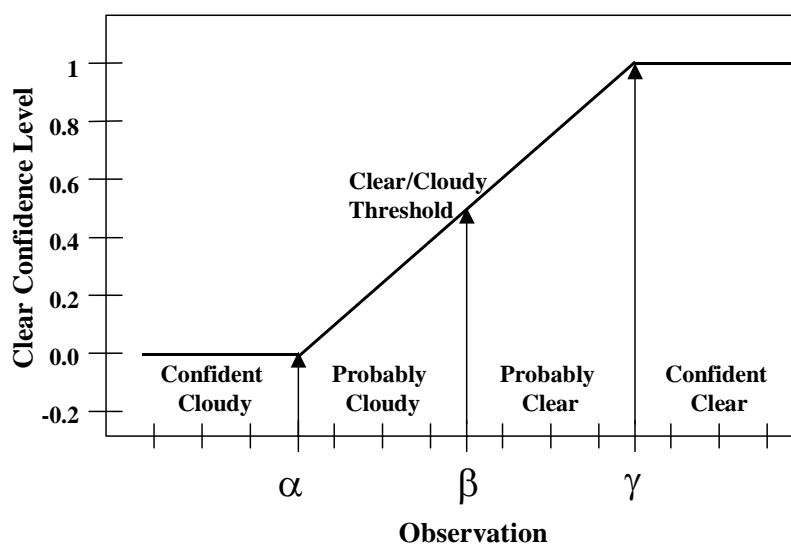
Figure 6. A graphical depiction of three thresholds used in cloud screening.

3.5 THEORETICAL DESCRIPTION OF CLOUD DETECTION

This section discusses the physics of detecting clouds using multispectral radiances and performing BT and Reflectance tests.

3.5.1 Physics of the Problem

Clouds are generally characterized by higher reflectance and lower temperature than the underlying earth surface. As such, simple visible and infrared window threshold approaches offer considerable skill in cloud detection. However, there are many surface conditions when this characterization of clouds is inappropriate, most notably over snow and ice. Additionally, some cloud types such as thin cirrus, low stratus at night, and small cumulus are difficult to detect because of insufficient contrast with the surface radiance. Cloud edges cause further difficulty since the instrument FOV will not always be completely cloudy or clear.

3.5.2 Infrared Brightness Temperature Threshold and Difference Tests

Several infrared window threshold and temperature difference techniques have been developed for cloud detection. These algorithms are described below.

3.5.2.1 IR Threshold Cloud Test (BT$_{M15}$)

The first infrared test to apply over the oceans is a simple threshold test. Over open ocean when BT$_{M15}$ is less than 270K, we assume the pixel to fail the clear-sky condition. With reference to Figure 6, the three thresholds over ocean are 267K, 270K, and 273K, respectively, as shown in Figure 7.
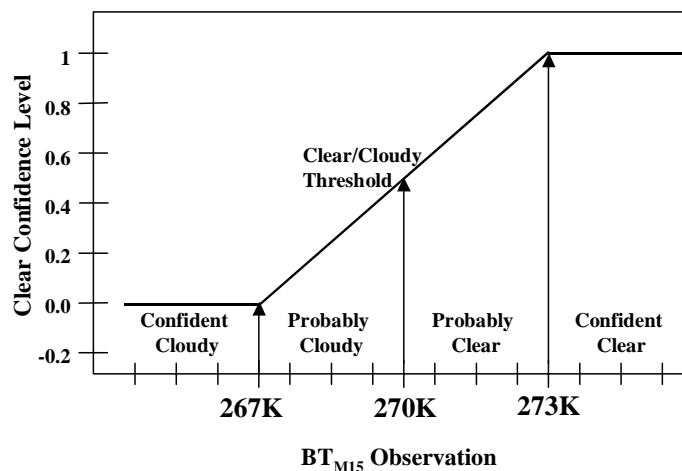
Figure 7. Thresholds for the simple IR window cold cloud test.

Cloud masking over land surface from thermal infrared bands is more difficult than over ocean due to potentially larger variations in surface emittance. Nonetheless, simple thresholds can be established over certain land features. For example, over arid desert regions we can expect that BT_{M15}< 292.5K denotes cloud. Such simple thresholds will vary with ecosystem, season, and time of day. Table 4 lists the thresholds used for the BT_{M15} test.

Table 4. Thresholds used for BT_{M15} test for cloud in the VCM algorithm

BT_{M15}			
Surface	**Confident Cloudy**	**Clear/Cloudy Threshold**	**Confident Clear**
Day Ocean	267.0	270.0	273.0
Day Desert (arid)	292.5	297.5	302.5
Day Desert (bright)	287.5	292.5	302.5
Night Ocean	267.0	270.0	273.0

3.5.2.2 Tri-Spectral Cloud Test ($BT_{M14} - BT_{M15}$ & $BT_{M15} - BT_{M16}$)

As a result of the relative spectral uniformity of surface emittance in the IR, spectral tests within various atmospheric windows (such as bands M14, M15, and M16 at 8.55μm, 10.76μm, and 12.01μm, respectively) can be used to detect the presence of cloud. Differences between BT_{M15} and BT_{M16} are widely used for cloud screening with AVHRR measurements, and this technique is often referred to as the split window technique. Saunders and Kriebel (1988) used BT_{M15}-BT_{M16} differences to detect cirrus clouds. Brightness temperature differences are greater over thin clouds than over clear or overcast conditions. Cloud thresholds are set as a function of satellite zenith angle and BT_{M15}.

In difference techniques, the measured radiances at two wavelengths are converted to brightness temperatures and subtracted. Because of the wavelength dependence of optical thickness and the non-linear nature of the Planck function (B_λ), the two brightness temperatures are often different.

The basis of the split window and tri-spectral technique for cloud detection lies in the differential water vapor absorption that exists between different window channel bands (M14 and M15 vs. M15 and M16). These spectral regions are considered to be part of the atmospheric window, where absorption is relatively weak. Most of the absorption lines are a result of water vapor molecules, with a minimum occurring within the M15 band. Since the absorption is weak, BT_{M15} can be corrected for moisture absorption by adding the scaled brightness temperature difference of two spectrally close channels with different water vapor absorption coefficients; the scaling coefficient is a function of the differential water vapor absorption between the two channels.

VIIRS has a unique capability since it has measurements at three wavelengths in the window 8.55μm, 10.76μm, and 12.01μm. The three spectral regions mentioned are very useful in determination of cloud free atmospheres. Because the index of refraction varies quite markedly over this spectral region for water, ice, and minerals common to many naturally occurring aerosols, the effect on the brightness temperature of each of the spectral regions is different, depending on the absorbing constituent.

Ackerman et al. (1990) suggested a tri-spectral combination of observations similar to those from M14, M15 and M16 for detecting cloud properties. Strabala et al. (1994) further explored this technique by utilizing very high spatial-resolution data from MAS. The physical premise of the technique is that ice and water vapor absorption peak in opposite halves of the window region; so that positive M14-M15 brightness temperature differences indicate cloud while negative differences, over oceans, indicate clear regions. The relationship between the two brightness temperature differences and clear-sky have also been examined using collocated HIRS and AVHRR GAC global ocean data sets. As the atmospheric moisture increases, $BT_{M14} - BT_{M15}$ decreases while $BT_{M15} - BT_{M16}$ increases.

Figure 8 demonstrates a relationship between $BT_{M15} - BT_{M16}$ and $BT_{M14} - BT_{M15}$ using MODIS observations over the Atlantic Ocean. Given a value of $BT_{M14} - BT_{M15}$, to be clear, a pixel requires $BT_{M15} - BT_{M16}$ to fall within a certain range of values. The threshold for this test is based on the value of $BT_{M15} - BT_{M16}$ which varies for each pixel.
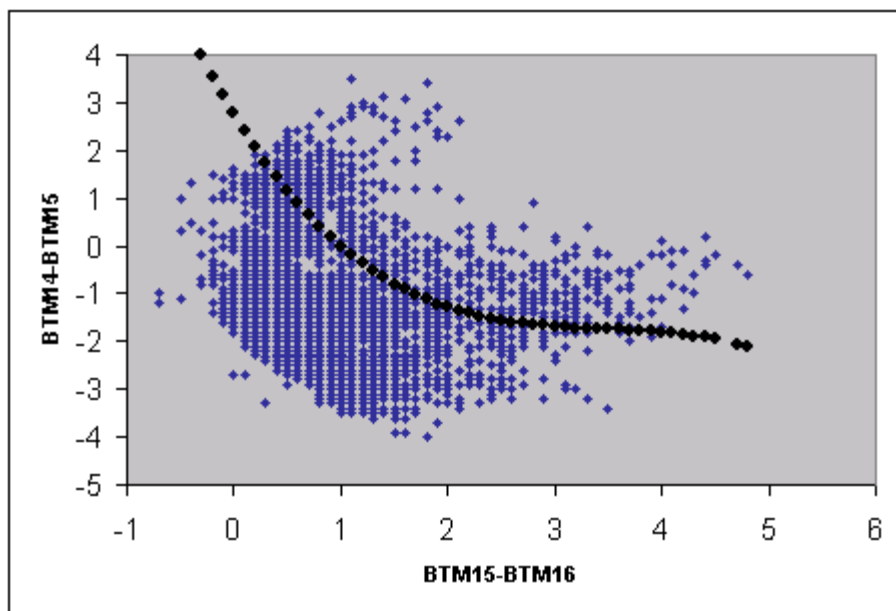

Figure 8. Tri-spectral diagram for ocean scenes taken from MODIS data. The dark diamonds in the figure represents the dynamic threshold for the tri-spectral test and the dark blue circles are the observed values. Values to the upper right of the threshold indicate cloud and lower left of the threshold indicate clear.

Brightness temperature difference testing can also be applied over land with careful consideration of variation in spectral emittance. For example, $BT_{M15} - BT_{M14}$ has large negative values over daytime desert and is driven to positive differences in the presence of cirrus. Some land regions have an advantage over ocean regions because of the larger number of surface observations, including air temperature and vertical profiles of moisture and temperature.

Table 5. Thresholds used for $BT_{M14} - BT_{M15}$ & $BT_{M15}-BT_{M16}$ test for cloud in the VCM algorithm

$BT_{M14}-BT_{M15}$ & $BT_{M15}-BT_{M16}$			
Surface	**Confident Cloudy**	**Clear/Cloudy Threshold**	**Confident Clear**
Day Ocean	Dynamic		
Night Ocean	Dynamic		

3.5.2.3 Cloud Test $(BT_{M15} - BT_{M12})$

The difference between BT_{M15} and BT_{M12} can be used to detect the presence of clouds. At night the difference between the brightness temperatures measured in the shortwave (3.7μm) and in the longwave (10.76μm) window regions can be used to detect partial cloud or thin cloud within the VIIRS FOV. Small or negative differences are observed only for the case where an opaque scene (such as thick cloud or the surface) fills the FOV of the sensor. Negative differences occur at night over extended clouds due to the lower cloud emissivity at 3.7μm.

During the daylight hours the difference between BT_{M15} and BT_{M12} is large and negative because of reflection of solar energy at M12. This technique is very successful at detecting low-level water clouds. Thresholds will vary for ecosystem type.

Moderate to large differences between BT_{M15} and BT_{M12} result when a non-uniform scene (e.g., broken cloud) is observed. The different spectral responses to a scene of non-uniform temperature are a result of Planck's law. The brightness temperature test is dependent on the temperature in the warmer portion of the scene increasing with decreasing wavelength (the shortwave window Plank radiance is proportional to the temperature to the thirteenth power, while the longwave dependence is to the forth power). Differences in the brightness temperatures of the longwave and shortwave channels are small when viewing mostly clear or mostly cloudy scenes; however, for intermediate situations the differences become large (greater than 3 degrees). Table 6 lists the thresholds used, which are of MODIS heritage.

Table 6. Thresholds used for $BT_{M15} - BT_{M12}$ test for cloud in the VCM algorithm

$BT_{M15}-BT_{M12}$			
Surface	**Confident Cloudy**	**Clear/Cloudy Threshold**	**Confident Clear**

BT$_{M15}$-BT$_{M12}$			
Surface	**Confident Cloudy**	**Clear/Cloudy Threshold**	**Confident Clear**
Day Land & Coast	-14.0	-12.0	-10.0
Day Ocean	-10.0	-8.0	-6.0
Day Desert (arid)	-20.0	-18.0	-16.0
Day Desert (bright)	-2.0	0.0	2.0
Night Land	3.0	2.5	2.0
Night Ocean	1.0	0.0	-1.0
Day Snow (high elevation)*	14.0	10.0	6.0
Day Snow (low elevation)*	10.0	7.0	4.0
Night Snow (low elevation)	0.70	0.60	0.50

*This test is BT$_{M12}$-BT$_{M15}$.

Infrared window tests at high latitudes are difficult. Distinguishing clear and cloud regions from satellite IR radiances is a challenging problem due to the cold surface temperatures. Yamanouchi et al. (1987) describes a nighttime polar (Antarctic) cloud/surface discrimination algorithm based upon brightness temperature differences between the AVHRR 3.7 and 11µm channels and between the 11 and 12µm channels. Their cloud/surface discrimination algorithm was more effective over water surfaces than over inland snow-covered surfaces. A number of problems arose over inland snow-covered surfaces. First, the temperature contrast between the cloud and snow surface became especially small, leading to a small brightness temperature difference between the two infrared channels. Second, the AVHRR channels are not well calibrated at extremely cold temperatures (< 200 K).

3.5.2.4 Cloud Detection Test (BT$_{M12}$ – BT$_{M13}$)

Performing this BT difference test is another method of separating the solar and thermal contributions of M12. Due to the small wavelength differences between these two bands the thermal contribution due to temperatures within a pixel are relatively close. The largest difference between these two bands is the solar component in the 3.7 µm channel. The difference removes the thermal emission, resulting in the solar component of 3.7 µm alone. Due to both the low reflectance of most surface types and the relative high reflectance of clouds in the 3.7 µm channel this test has demonstrated much promise in MAS data. Table 7 lists the thresholds used in the BT$_{M12}$-BT$_{M13}$ test.

Table 7. Thresholds used for BT$_{M12}$ – BT$_{M13}$ test for cloud in the VCM algorithm

BT$_{M12}$-BT$_{M13}$			
Surface	**Confident Cloudy**	**Clear/Cloudy Threshold**	**Confident Clear**

Raytheon

BT$_{M12}$-BT$_{M13}$			
Surface	**Confident Cloudy**	**Clear/Cloudy Threshold**	**Confident Clear**
Day Land	10.5	10	9.5
Day Ocean	6.5	6	5.5
Day Snow	8.5	8	7.5

3.5.3   Visible Reflectance Tests

3.5.3.1 Visible Reflectance (M5 & M7)

The visible reflectance test is a single channel test whose strength is discriminating bright clouds over dark surfaces (e.g., stratus over ocean) and weakness is clouds over bright surfaces (e.g., snow). Two different channels are used in this test dependent on the ecosystem. Band M5 (0.67 μm) is used over land and snow/ice regions. The M7 (0.87 μm) reflectance test is applied over oceans and desert scenes. The nominal thresholds are given below. These thresholds are set based on observations from AVHRR and MAS and are listed in Tables 8 and 9.

Table 8. Thresholds used for Ref$_{M5}$ test for low cloud in the VCM algorithm

Ref$_{M5}$			
Surface	**Confident Cloudy**	**Clear/Cloudy Threshold**	**Confident Clear**
Day Land & Coast & Snow	0.22	0.18	0.14

Table 9. Thresholds used for Ref$_{M7}$ test for cloud in the VCM algorithm

Ref$_{M7}$			
Surface	**Confident Cloudy**	**Clear/Cloudy Threshold**	**Confident Clear**
Day Ocean	0.065	0.055	0.045
Day Desert	0.34	0.30	0.26

3.5.3.2 Visible Reflectance Ratio Test (M7/M5)

The reflectance ratio test uses channel M7 divided by channel M5 (Ref$_{0.865\mu m}$ /Ref$_{0.672\mu m}$). This test makes use of the fact that the spectral reflectance at these two wavelengths is similar over clouds (ratio is near 1) and different over water and vegetation. Using AVHRR data this ratio has been found to be between 0.9 and 1.1 in cloudy regions over ocean. If the ratio falls within this range, a cloud is indicated. Since the threshold is a range of numbers, there are six threshold values for this test over ocean – three surrounding the upper limit value (high) and three surrounding the lower limit value (low). Adjustments to the ratio thresholds listed in Table 10 will be made as necessary for VIIRS data and must be a function of the ecosystem as noted below.

Table 10. Thresholds used for Ref$_{M7}$/Ref$_{M5}$ test for cloud in the VCM algorithm

Ref$_{M7}$/Ref$_{M5}$			
Surface	Confident Cloudy	Clear/Cloudy Threshold	Confident Clear
Day Land	1.85	1.90	1.95
Day Ocean (high)	0.95	1.10	1.15
Day Ocean (low)	0.95	0.90	0.85

Figure 9 illustrates some of the complexities of desert ecosystems as demonstrated by the visible reflectance ratio. The observations are from the AVHRR on the NOAA-9 and are over the Arabian Sea, the Arabian Peninsula, and surrounding regions. The figure shows histograms of reflectance ratio values for coastal/water scenes, as well as desert and more densely vegetated areas in the Persian Gulf region from approximately 15-25° N latitude and 50-70° E longitude. Almost all of the observations recorded in the histograms were from clear-sky conditions, as determined by inspection of visible and IR imagery. As suggested by the histograms of Ref$_{M7}$/Ref$_{M5}$, clear-sky ocean scenes have a ratio of less than 0.75. The surface type classifications are from the Olson World Ecosystems data set. One can immediately see that clear-sky desert values of the visible reflectance ratio cover a large range of values, including values one might normally associate with cloudy skies over vegetated surfaces. Also note the large amount of overlap between the desert and shrub/grassland categories. This figure shows that clear-sky spectral threshold tests need to be applied very carefully in arid regions and also points out the need for high-resolution ecosystem maps. This test will not be performed over desert, semi-desert, snow/ice, or some agricultural ecosystems. In addition to land, this reflectance ratio test may be performed over water during the daytime. When applied in regions of possible sun glint, an angular dependence is included in the thresholds. These thresholds are based on analysis of AVHRR LAC and GAC data and the APOLLO algorithm.
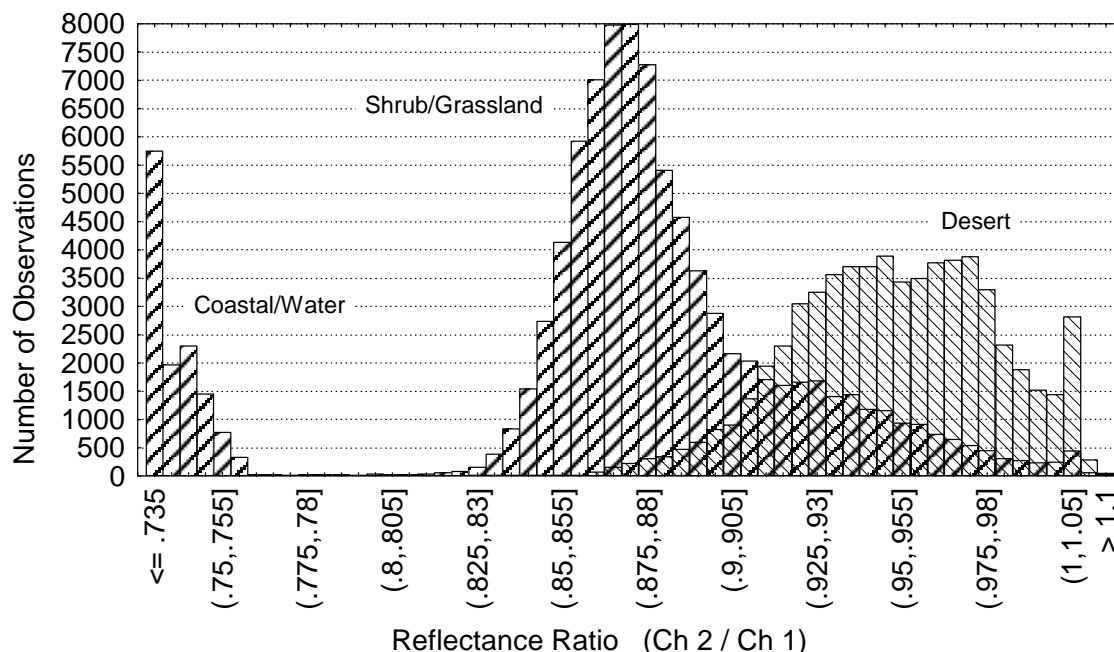
Raytheon

Figure 9. Histogram of the frequency of occurrence of the AVHRR reflectance ratio R0.86/R0.63 for a scene over the Arabian Peninsula and Arabian Sea

3.5.4 Thin Cirrus Tests

3.5.4.1 Visible (Ref$_{M9}$)

VIIRS band M9 (1.38 μm) will use reflectance thresholds on a per pixel basis to detect the presence of thin cirrus cloud in the upper troposphere under daytime viewing conditions. The strength of this cloud detection channel lies in the strong water vapor absorption in the 1.38 μm region. With sufficient atmospheric water vapor present (estimated to be about 0.4 cm precipitable water) in the beam path, no upwelling reflected radiance from the Earth's surface reaches the satellite. Since 0.4 cm is a small atmospheric water content, most of the earth's surface will indeed be obscured in this channel. With relatively little of the atmosphere's moisture located high in the troposphere, high clouds appear bright; reflectance from low and mid level clouds is partially attenuated by water vapor absorption.

Simple low and high reflectance (normalized by incoming solar at the top of the atmosphere) thresholds will be used to separate thin cirrus from clear and thick (near infrared cloud optical depth > ~ 0.2) cloud scenes. Ben-Dor (1994) analyzed a scene from the Airborne Visible Infrared Imaging Spectrometer (AVIRIS) to demonstrate that thin cirrus detection using 1.38 μm observations may be more difficult for elevated surfaces, dry atmospheric conditions, and high albedo surfaces. New injections of volcanic aerosols into the stratosphere may also impact this test.

If the reflectance is greater than the clear-sky threshold and less than a thick cloud, then the thin cirrus bit will indicate thin cirrus detected. We subjectively define thin cirrus as a cloud that has

a small impact on the visible reflectance, enabling atmospheric correction to be applied to retrieve land surface properties (i.e., NDVI). Given the sensitivity to thin high clouds, the VIIRS 1.38 μm channel may detect much larger cloud coverage than previous satellite algorithms have indicated. Table 11 lists the thresholds used for the Ref_{M9} test.

Table 11. Thresholds used for Ref_{M9} test for cirrus cloud in the VCM algorithm

Ref_{M9}			
Surface	Confident Cloudy	Clear/Cloudy Threshold	Confident Clear
Day Land, Coastal, Ocean, Desert, Snow	0.040	0.035	0.030

3.5.4.2 Infrared (BT_{M15}-BT_{M16})

This BT difference test is used to detect cirrus clouds during the day and night over a variety of surfaces. The thresholds are dependent on the satellite zenith angle and BT_{M15} (Saunders and Kriebel, 1988). Table 12 details which scenes the test is executed and Table 13 lists the clear/cloudy Look-Up Table for this test in mid-latitudes. To obtain the clear/cloudy threshold for this test, a bi-dimensional linear interpolation of values in Table 13 must be performed. The confident cloudy threshold can be found by adding an incremental quantity to the clear/cloudy threshold, and the confident clear threshold can by found by subtracting the incremental quantity from the clear/cloudy threshold.

Table 12. Scenes where the BTM15-BTM16 test will be executed

BT_{M15}-BT_{M16}
Day Land
Day Coastal
Day Ocean
Day Desert
Night Land
Night Ocean

Table 13. Clear/Cloudy temperature thresholds in Kelvin for BT_{M15}-BT_{M16} cloud detection test at mid-latitudes

BT_{M15}	secant(satellite zenith angle)				
	1.0	**1.25**	**1.50**	**1.75**	**2.0**
260K	0.55	0.60	0.65	0.90	1.10
270K	0.58	0.63	0.81	1.03	1.13

BT_{M15}	secant(satellite zenith angle)				
	1.0	**1.25**	**1.50**	**1.75**	**2.0**
280K	1.30	1.61	1.88	2.14	2.30
290K	3.06	3.72	3.95	4.27	4.73
300K	5.77	6.92	7.00	7.42	8.43
310K	9.41	11.22	11.03	11.60	13.39

3.5.4.3 High Cloud Test ($BT_{M12} - BT_{M16}$)

This window brightness temperature difference test is applied during the nighttime over land and snow surfaces. This difference is useful for separating thin cirrus from cloud free condition and is relatively insensitive to the amount of water vapor in the atmosphere (Hutchison and Hardy 1995).

Table 14. Thresholds used for $BT_{M12} - BT_{M16}$ test for high cloud in the VCM algorithm

BT_{M12}-BT_{M16}			
Surface	**Confident Cloudy**	**Clear/Cloudy Threshold**	**Confident Clear**
Night Land	4.50	4.00	3.50
Night Snow	4.50	4.00	3.50

3.5.5 Cloud Confidence

Each of the tests above returns a confidence level ranging from 0 (high confidence that the pixel is cloudy) to 1 (high confidence that the pixel is clear). The individual confidence levels must be combined to determine a final decision on clear or cloudy. We shall denote the confidence level of an individual test as F_i and the final quality flag as Q.

The VIIRS Cloud Mask is a clear-sky conservative case. A test with a confident clear result sets the bit to clear. Several tests are not independent of one another. For example, consider daytime over oceans in regions without sun glint. If stratocumulus clouds are present, they will likely be detected by the visible reflectance test, the reflectance ratio test, and BT_{M15}-BT_{M12}. These same tests will likely miss the presence of thin uniform cirrus clouds, which would probably be detected by the tri-spectral test (combinations of BT_{M14}, BT_{M15}, and BT_{M16}). Very thin cirrus clouds would best be detected by the Ref_{M9} test, which has difficulty detecting low-level clouds. Because of this overlap in the type of clouds different tests detect, each test is considered in one of five groups. The five groups are:

Group I (Emission Threshold)

       BT_{M15}

Group II (Emission Difference)

      BT_{M12}-BT_{M13}

      BT_{M15}-BT_{M12}

      BT_{M14}-BT_{M15} & BT_{M15}-BT_{M16}

Group III (Reflectance Threshold)

      Ref_{M5}

      Ref_{M7}

      Ref_{M7}/Ref_{M5}

Group IV (Reflectance Thin Cirrus)

      Ref_{M9}

Group V (Emission Thin Cirrus)

      BT_{M15}-BT_{M16}

      BT_{M12}-BT_{M16}

A minimum confidence is determined for each group,

$$G_{i=1,5} = \min[F_i].$$

The final cloud mask is then determined from the product of the results from each group;

$$Q = \sqrt[5]{\prod_{i=1}^{5} G_i} \ .$$

This approach is considered clear-sky conservative. If any test is highly confident that the scene is cloudy ($F_i = 0$), the final cloud mask is $Q = 00$, which is confident cloudy.

The algorithm is divided into eight conceptual domains according to surface type and solar illumination:

1. Daytime land
2. Daytime coast
3. Daytime water
4. Daytime desert
5. Daytime snow/ice covered regions
6. Nighttime land
7. Nighttime water
8. Nighttime snow/ice covered regions.

Raytheon

"Daytime" is defined as a solar zenith angle $\theta_0 < 85°$. The "desert" classification is based on the USGS Global Ecosystem map. For all observations within a given domain, it is generally expected that: (i) the same tests may be performed, and (ii) threshold values for each of these tests will not change. It is expected that more domains may be established in the future.

3.6 PRACTICAL CONSIDERATIONS

3.6.1 Numerical Computation Considerations

Bispectral cloud detection tests are computationally inexpensive. All possible cloud detection tests will be applied for a given pixel. Tests for aerosols, shadows, and fire are made only after all cloud tests have been applied and pixels identified as cloud-contaminated have been flagged.

3.6.2 Programming and Procedural Considerations

The procedural outline has been described in Section 3.1.

3.6.3 Configuration of Retrievals

To avoid "hard-wiring" specific values into the operational software, a retrieval configuration file can be adopted. The file would store numerical values of adjustable parameters used within the retrievals, such as the thresholds establishing whether a successful retrieval occurs.

3.6.4 Quality Assessment and Diagnostics

The first 4 bits of the VIIRS Cloud Mask output make up a quality indicator. Additional information regarding the VIIRS Cloud Mask quality can be found in Section 3.3.1.

3.6.5 Exception Handling

VIIRS will produce a cloud mask under all circumstances. If a band is bad, the tests that use that band will not be used. This will be reflected in the Cloud Mask Quality flag.

3.7 ALGORITHM VALIDATION

The VIIRS cloud mask algorithm will be verified pre-launch using data from existing satellite systems, such as Advanced Very High Resolution Radiometer (AVHRR) and MODIS. More pre-launch validation will be performed along with the update of detection modules. Post-launch verification will involve intercomparisons between VIIRS observations, ground-based measurements, and special airborne campaigns.

3.8 ALGORITHM DEVELOPMENT SCHEDULE

The algorithm for the VIIRS cloud mask is of MODIS heritage, with the exception an additional BTD test not found in the MODIS algorithm. The methods will be verified using MODIS global data as it becomes available. The similarity of the proposed VIIRS bands to the MODIS bands makes MODIS data a reliable verification source.

4.0 ASSUMPTIONS AND LIMITATIONS

4.1 ASSUMPTIONS

(1)   Cloud Mask receives an image of VIIRS calibrated and geolocated TOA reflectances and TOA BT's in the bands used by the Cloud Mask, including any Imagery bands used.

(2)   Quality flags accompany all input data into the Cloud Mask Module indicating if the data is good or questionable.

(3)   Cloud Mask receives Geolocated Latitudes and Longitudes of all pixels in the region being masked.

(4)   Cloud Mask receives an entire image of the region being masked.

(5)   Cloud Mask needs a Land/Water reference database.

(6)   Cloud Mask needs an Ecosystem reference database.

(7)   Cloud Mask receives Sun Sensor geometry.

(8)   Cloud Mask receives a database of recent snow/ice knowledge.

(9)   Cloud Mask receives sea surface wind speed data in region being masked for determination of Sun Glint Flag.

(10)   Output mask results will have 4 levels of confidence: Confident Cloudy, Probably Cloudy, Probably Clear, and Confident Clear.

4.2 LIMITATIONS

(1)   Can only produce Cloud Mask if BT and Reflectance data are available.

(2)   Can only produce Cloud Mask if underlying surface type is known.

5.0 REFERENCES

Ackerman, S. A., W. L. Smith and H. E. Revercomb (1990). The 27-28 October 1986 FIRE IFO Cirrus Case Study: Spectral Properties of Cirrus Clouds in the 8-12 Micron Window. *Mon. Wea. Rev.*, 118, 2377-2388.

Ackerman, S. A., (1996). Global satellite observations of negative brightness temperature difference between 11 and 6.7 µm. *J. Atmos. Sci.*, 53, 2803-2812.

Ackerman, S. A., K. Strabala, P. Menzel, R. Frey, C. Moeller, L. Gumley, B. Baum, C. Schaaf, and G. Riggs (1997). Discriminating Clear-Sky From Cloud With MODIS Algorithm Theoretical Basis Document (MOD35). Version 3.2

Baum, B.A., P.F. Soulen, K.I. Strabala, M.D. King, S.A. Ackerman, W.P. Menzel, and P. Yang, (2000). Remote Sensing of Cloud Properties Using MODIS Airborne Simulator Imagery During SUCCESS. II. Cloud Thermodynamic Phase, *J. Geophys. Res., 9,* 11781-11792, 2000.

Ben-Dor, E., (1994). A precaution regarding cirrus cloud detection from airborne imaging spectrometer data using the 1.38 µm water vapor band. *Remote Sens. Environ.*, 50, 346-350.

Berk, A., L. S. Bernstein, and D. C. Roberson (1989). MODTRAN: A Moderate Resolution Model for LOWTRAN7, Report AFGL-TR-89-0122 (Air Force Geophysics Laboratory), Hanscom, AFB, MA 01731.

Gao, B. C., A. F. H. Goetz, and W. J. Wiscombe (1993). Cirrus Cloud Detection From Airborne Spectrometer Data Using the 1.38 Micron Water Vapor Band, *Geophys. Res. Lett.*, 20, 301-304.

Goodman, A. H., and A. Henderson-Sellers (1988). Cloud Detection Analysis: A Review of Recent Progress. *Atm. Res.*, 21, 203.

Gustafson, G. B., R. G. Isaacs, R. P. d'Entremont, J. M. Sparrow, T. M. Hamill, C. Grasotti, D. W. Johnson, C. P. Sarkisian, D. C. Peduzzi, B. T. Pearson, V. D. Jakabhazy, J. S. Belfiore, and A. S. Lisa (1994). Support of Environmental Requirements for Cloud Analysis and Archive (SERCAA): algorithm descriptions, PL-TR-94-2114, Phillips Laboratory, AFMC, Hanscom AFB, MA.

Hall, D. K., G. A. Riggs, and V. V. Solomonson (1995). Development of Methods for Mapping Global Snow Cover Using Moderate Resolution Imaging Spectroradiometer Data. *Remote Sens. Env.*, 54, 127-140.

Hall, D. K., G. A. Riggs, and V. V. Solomonson (1996). Algorithm Theoretical Basis Document (ATBD) for the MODIS Snow-, Lake Ice-, and Sea Ice-Mapping Algorithms. Version 3.0.

Hutchison, K. D., and K. Hardy (1995). Threshold functions for automated cloud analyses of global meteorological satellite imagery. *International Journal of Remote Sensing,* 16, 3665-3680.

Hutchison, K. D., and N. Choe (1996). Application of 1.38 μm imagery for thin cirrus detection in daytime imagery collected over land surfaces. *International Journal of Remote Sensing,* 17, 3325-3342.

Hutchison, K. D., and J. K. Locke (1997). Snow Identification through Cirrus Cloudy Atmospheres using AVHRR Daytime Imagery. *Geophysical Research Letters*, 24, 1791-1794.

Hutchison, K. D., B. J. Etherton, and P. C. Topping (1997). Validation of automated cloud top phase algorithms: distinguishing between cirrus clouds and snow in a-priori analyses of AVHRR imagery. *Optical Engineering*., 36, 1727-1737.

Hutchison, K. D., B. J. Etherton, P. C. Topping, and A. H. L. Huang (1997). Cloud Top Phase Determination from the Fusion of Signatures in Daytime AVHRR Imagery and HIRS Data. *International Journal of Remote Sensing*, 18, 3245-3262.

Hutchison, K. D., K. Hardy, and B. C. Gao (1995). Improved detection of optically-thin cirrus clouds in nighttime multispectral meteorological satellite imagery using total integrated water vapor information. *Journal of Applied Meteorology,* 34, 1161-1168.

Inoue, T., (1987). A cloud type classification with NOAA 7 split window measurements. *J. Geophys. Res*., 92, 3991-4000.

King, M. D., W. P. Menzel, P. S. Grant, J. S. Myers, G. T. Arnold, S. E. Platnick, L. E. Gumley, S. C. Tsay, C. C. Moeller, M. Fitzgerald, K. S. Brown, and F. G. Osterwisch (1996). Airborne Scanning Spectrometer for Remote Sensing of Cloud, Aerosol, Water Vapor, and Surface Properties. *J. Atmos. Oceanic Technol*., 13, 777-794.

Kriebel, K. T., and R. W. Saunders (1988). An Improved Method for Detecting Clear Sky and Cloudy Radiances from AVHRR Data. *Int. J. Remote Sens*., 9, 123-150.

Lou, G., P. A. Davis, L. L. Stowe, and E. P. Mcclain (1995). A pixel-scale algorithm of cloud type, layer, and amount for AVHRR data. Part I: Nighttime, *Journal of Atmospheric and Oceanic Technology*, 12, 1014-1036.

McClain, C. R. and Yeh, E.-N. (1994). Sun Glint Flag Sensitivity Study, SeaWiFS Technical Report Series, 13, Case Studies for SeaWiFS Calibration and Validation, Part 1, 46-47.

Rossow, W. B. (1989). Measuring Cloud Properties from Space: A Review. *J. Clim*., 2, 201.

Saunders, R. W. and K. T. Kriebel, (1988). An improved method for detecting clear sky and cloudy radiances from AVHRR data, *International Journal of Remote Sensing,* 9, 123-150.

Raytheon

Stamnes, K., W. Li, X. Xiong, and B. Chen (1998). Remote Sensing of Cloud and Surface Properties in Polar Regions from GLI Measurements on Board ADEOS-II. The 3rd GLI Workshop, Tokyo.

Stowe, L. L., P. Davis, and E. P. McClain (1995). Evaluating CLAVR (Clouds from AVHRR) Phase I Cloud Cover Experimental Product. *Adv. in Space Res.*, 16, 21-24.

Stowe, L. L., P. Davis, and E. P. McClain (1998). Scientific Basis and Initial Evaluation of the CLAVR-I Global Clear/Cloud Classification Algorithm for the Advanced Very High Resolution Radiometer, *J. Atmos. and Oceanic Technology*, submitted May 1st.

Strabala, K. I., S. A. Ackerman, and W. P. Menzel (1994). Cloud Properties Inferred from 12 micron Data, *J. Appl. Meteor.*, 33, 212-229.

Valvocin, F. R. (1978). Spectral radiance of snow and clouds in the near infrared spectral region. *Tech Report No. 78-0289*, Air Force Geophysics Laboratory, Hanscom Air Force Base, MA.

Yamanouchi, T., K. Suzuki, and S. Kawaguci, (1987). Detection of clouds in Antarctica from infrared multispectral data of AVHRR. *J. Meteor. Soc. Japan*, 65, 949-962.